doi:10.1017/S1431927620016505
Microsc. Microanal. 26 (Suppl 2), 2020

Angle-Resolved Electron Energy Loss Spectroscopy

Tracy Lovejoy[1], Benjamin Plotkin-Swing[1], Niklas Dellby[1], Chris Meyer[1], Andreas Mittelberger[1], Alberto Eljarrat[2], Benedikt Haas[2], Christoph Koch[2] and Ondrej Krivanek[1]

[1]Nion Co., Kirkland, Washington, United States, [2]Humboldt-Universität zu Berlin, Berlin, Berlin, Germany

Angle-Resolved Electron Energy Loss Spectroscopy (AREELS) is a field with rich history. Early Möllenstedt, Castaing-Henry and Wien analyzers were able to analyze electron scattering in energy along one axis, and in angle (or position) along a perpendicular axis on their 2D detectors (silver halide plates). In other words, they could record S(q,w) patterns rather than angle-integrated EEL spectra. By 1975, the angular dependence of Cerenkov radiation, guided optical modes, and surface and bulk plasmons had been recorded and explained theoretically [1]. The advent of vibrational spectroscopy in the electron microscope [2], combined with the ability to distinguish different vibrational modes by their characteristic angular dependence, has recently led to a major resurgence of interest in AREELS [3-5].

Much of the progress has been made possible by monochromators and spectrometers [6] that allow EELS energy resolution of 5 meV and better to be reached. The instrumentation has advanced further through the introduction of hybrid-pixel detectors for EELS [7], which allow the intense zero loss peak (ZLP), typically containing 3-300 pA current, to be recorded without saturation. At the same time, single electron arrivals are recorded without significant read-out noise, and reaching $>10^7$:1 dynamic range in spectra and S(q,w) patterns is now routine. The detectors also minimize the sideways spread of the ZLP – another key requirement for artifact-free recording of S(q,w) patterns.

Fig. 1 shows two experimental S(q,w) patterns recorded from a hexagonal BN flake. The h-BN c-axis was parallel to the electron beam, and an EELS entrance slit selected scattering events along the directions in the diffraction pattern indicated in Fig. 1(c). Similar to S(q,w) patterns recorded with a scintillator-based SCMOS camera reported previously [8], the slit was 125 μm wide and 2.0 mm long. The diffraction patterns were rotated as needed using the post-sample lenses of the microscope column, whose principal effect at weak excitations is to rotate the beam. Other key parameters were as follows: Nion HERMES and Iris EELS, Dectris ELA hybrid-pixel direct detector, primary energy 60 keV, monochromator slit set to about 5 meV energy width, 4 pA beam current incident on the sample, incident beam convergence semi-angle ~2 mrad. For Fig. 1(a), 240 separate exposures of 4 sec each were recorded and summed, for a total acquisition time of 16 min; for Fig. 1(b), 120 exposures of 4 sec were summed (8 min total). The patterns were aligned in energy prior to the summation, and energy shifts of individual columns due to charging of the edges of the momentum-selecting slit were corrected too. Major charging was not correctable in this way and resulted in vertical streaks in the summed patterns, marked by green arrows in Fig. 1 (b). No other processing was performed. We are now developing procedures for the correction of major charging, and looking for slit materials less affected by it.

The dispersion branches have been labeled in accordance with theoretical simulations of Senga et al. [ref. 4, extended data Fig. 4], with which they show excellent correspondence. ZLP tails have been suppressed to an extent that energy losses at energies as low as 30 meV are visible without performing any background subtraction, and ***energy gain dispersion branches***, marked by dashed blue arrows, are readily distinguishable at room temperature.

The richness of the information available in Fig. 1 is striking, especially when it is compared to similar S(q,w) patterns acquired previously. The patterns were recorded with a beam about 2 nm in diameter, as sub-unit cell spatial resolution is not compatible with good angular resolution. Similar data should be obtainable at stacking faults, grain boundaries and other defects in many types of materials [5], leading to a local analysis of

vibrational properties not possible by any other experimental technique. Another promising possibility lies in recording S(q,w) patterns due to interband transitions in semiconductors and insulators, aiming to measure indirect band gaps and other transitions requiring non-zero momentum transfer. The intensity for this type of scattering falls off much faster with the scattering angle than phonon scattering, but the wide dynamic range of the hybrid pixel detector used here should make it possible to overcome this handicap.

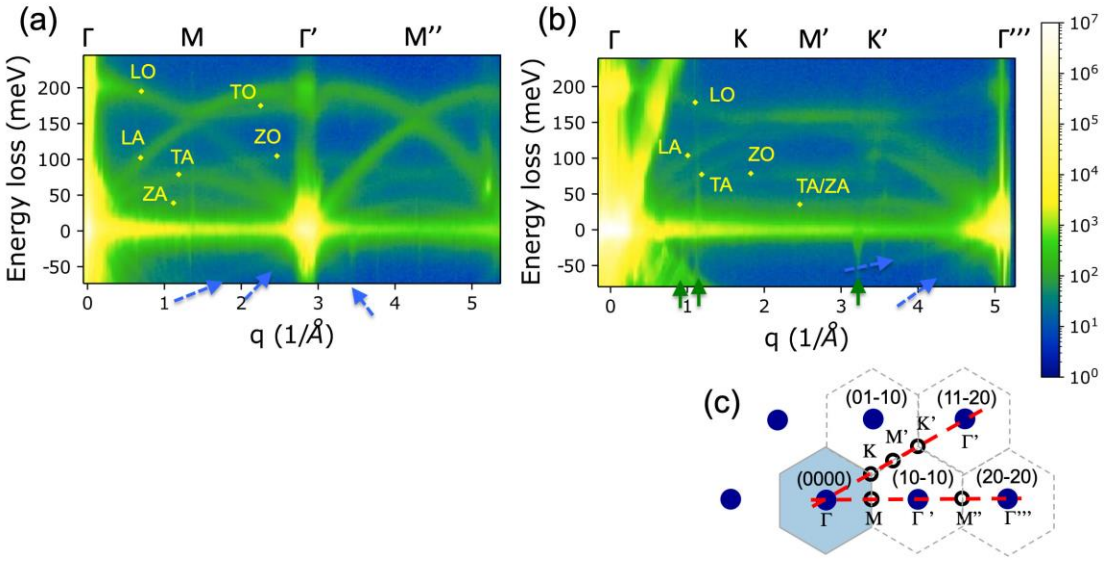

Figure 1. (a) Experimental S(q,w) pattern of BN along the G-M-G'-M''-G''' line. (b) S(q,w) pattern along G-K-M'-K'-G''. Dashed blue arrows indicate energy gain branches, short green arrows show artifacts due to slit charging. (c) Schematic diffraction pattern showing the first Brillouin zone (blue hexagon), higher order Brillouin zones, high-symmetry points in k-space, and the selection made by the EELS entrance slot. Nion HERMES, ELA direct detector, 60 keV.

References

1] C.H. Chen et al., Phys. Rev. **B12** (1975) 64.
[2] O.L. Krivanek et al., Nature **514** (2014) 209; T. Miata et al., Microscopy **63** (2014) 377.
[3] F.S. Hage et al., Sci. Adv. 2018;4:eaar7495 1-5.
[4] R. Senga et al., Nature **573**, (2019) 247.
[5] X. Yan et al., submitted (2020)
[6] T.C. Lovejoy et al., Microsc. Microanal. **24** (Suppl. 1, 2018) 446.
[7] B. Plotkin-Swing et al., these proceedings; full paper submitted to Ultramicroscopy (2020).
[8] A.L. Bleloch et al., Microsc. Microanal. **25** (Suppl. 2, 2019) 512.

https://doi.org/10.1017/S1431927620016505 Published online by Cambridge University Press